Bax, A., Griffith, R., & Hawkins, B. L. (1983) *J. Magn. Reson. 55*, 301.
Bax, A., Kay, L. E., Sparks, S. W., & Torchia, D. A. (1989) *J. Am. Chem. Soc. 111*, 408.
Bendell, M. R., Pegg, D. T., & Doddrell, D. M. (1983) *J. Magn. Reson. 52*, 81.
Bystrov, V. F. (1976) *Prog. Nucl. Reson. Spectrosc. 10*, 41-81.
Clore, G. M., & Gronenborn, A. M. (1987) *Protein Eng. 1*, 275-288.
Clore, G. M., & Gronenborn, A. M. (1989) *CRC Crit. Rev. Biochem. Mol. Biol. 24*, 479-564.
Clore, G. M., Bax, A., Wingfield, P., & Gronenborn, A. M. (1988) *FEBS Lett. 238*, 17-21.
Forman-Kay, J. D., Clore, G. M., Driscoll, P. C., Wingfield, P., Richards, F. M., & Gronenborn, A. M. (1989) *Biochemistry 28*, 7088-7097.
Gronenborn, A. M., Bax, A., Wingfield, P. T., & Clore, G. M. (1989a) *FEBS Lett. 243*, 93-98.
Gronenborn, A. M., Wingfield, P. T., & Clore, G. M. (1989b) *Biochemistry 28*, 5081-5089.
Karplus, M. (1963) *J. Am. Chem. Soc. 85*, 2870.
Kay, L. E., & Bax, A. (1990) *J. Magn. Reson.* (in press).
Kay, L. E., Brooks, B., Sparks, S. W., Torchia, D. A., & Bax, A. (1989) *J. Am. Chem. Soc. 111*, 1515-1516.
Marion, D., & Wüthrich, K. (1983) *Biochem. Biophys. Res. Commun. 113*, 967-974.
Marion, D., Kay, L. E., Sparks, S. W., Torchia, D. A., & Bax, A. (1989a) *J. Am. Chem. Soc. 111*, 1515-1516.
Marion, D., Driscoll, P. C., Kay, L. E., Wingfield, P. T., Bax, A., Gronenborn, A. M., & Clore, G. M. (1989b) *Biochemistry 28*, 6150-6156.
Neuhaus, D., Wagner, G., Vasák, M., Kägi, J. H. R., & Wüthrich, K. (1985) *Eur. J. Biochem. 151*, 257-273.
Pardi, A., Billeter, M., & Wüthrich, K. (1984) *J. Mol. Biol. 180*, 741-751.
Powell, M. J. D. (1965) *Comput. J. 7*, 303-307.
Wollman, E. E., d'Auriol, L., Rimsky, L., Shaw, A., Jacquot, J.-P., Wingfield, P., Graber, P., Dessarps, F., Robin, P., Galibert, F., Bertoglio, J., & Fradelizi, D. (1988) *J. Biol. Chem. 263*, 15506-15512.
Wüthrich, K. (1986) *NMR of Proteins and Nucleic Acids*, Wiley, New York.
Zuiderweg, E. R. P., & Fesik, S. W. (1989) *Biochemistry 28*, 2387-2391.

Environments and Conformations of Tryptophan Side Chains of Gramicidin A in Phospholipid Bilayers Studied by Raman Spectroscopy†

Hideo Takeuchi, Yasuhisa Nemoto,‡ and Issei Harada*
Pharmaceutical Institute, Tohoku University, Aobayama, Sendai 980, Japan
Received July 12, 1989; Revised Manuscript Received October 9, 1989

ABSTRACT: Raman spectroscopy has been used to investigate the hydrophobic interaction of the indole ring with the environments, the water accessibility to the N_1H site, and the conformation about the C_β–C_3 bond for the four tryptophan side chains of gramicidin A incorporated into phospholipid bilayers. Most of the tryptophan side chains of the head-to-head helical dimer transmembrane channel are strongly interacting with the lipid hydrocarbon chains, and the hydrophobic interactions for the rest increase with increasing hydrocarbon chain length of the lipid. One tryptophan side chain (probably Trp-15) is accessible to water molecules, another (Trp-9) is deeply buried in the bilayer and inaccessible, and the accessibilities of the remaining two (Trp-11 and Trp-13) depend on the bilayer thickness. The torsional angle about the C_β–C_3 bond is found to be ±90° for all the tryptophans irrespective of the membrane thickness. Binding of the sodium cation to the channel does not change the torsional angles but decreases the water accessibilities of two tryptophans (Trp-11 and Trp-13) considerably. In conjunction with a slight spectral change in the amide III region, it is suggested that the sodium binding causes a partial change in the main-chain conformation around Trp-11 and Trp-13, which results in the movements of these side chains toward the bilayer center. Two models consistent with the present Raman data are proposed for the tryptophan orientation in the dominant channel structure.

Gramicidin A is a linear pentadecapeptide composed of alternating L- and D-amino acids with the N- and C-terminal residues blocked by a formyl and an ethanolamide group, respectively: HCO-L-Val-Gly-L-Ala-D-Leu-L-Ala-D-Val-L-Val-D-Val-L-Trp-D-Leu-L-Trp-D-Leu-L-Trp-D-Leu-L-Trp-$NHCH_2CH_2OH$ (Sarges & Witkop, 1964). This peptide forms transmembrane channels that induce permeability to monovalent cations and water in natural and artificial lipid membranes (Hladky & Haydon, 1972; Myers & Haydon, 1972; Rosenberg & Finkelstein, 1978; Finkelstein & Andersen, 1981). The structure of the channel has been studied extensively by various physicochemical methods, and a model proposed by Urry (1971) for the backbone conformation is now generally accepted (Weinstein et al., 1980; Urry et al., 1982b, 1983; Wallace et al., 1986). According to the model, the channel is a dimer consisting of two left-handed β-helical

†Supported in part by a Grant-in-Aid for General Scientific Research (62570958) from the Ministry of Education, Science and Culture of Japan.
‡Present address: Department of Cell Biology, The Research Institute for Tuberculosis and Cancer, Tohoku University, Seiryo, Aoba, Sendai 980, Japan

0006-2960/90/0429-1572$02.50/0

monomers linked together at their N termini. The head-to-head dimerized helical conformation is stabilized by successive intramonomer and intermonomer hydrogen bonds from the amide NH groups to the amide or formyl C=O groups, while the amino acid side chains are directed from the central helical backbone outward to the membrane bilayer, leaving a tunnel for ion transport inside the helix.

In contrast to substantial evidence for the backbone structure, little is known about the conformations of the side chains and their interactions with membranes, which may be an important factor determining the channel activity. Four tryptophan side chains located in the C-terminal half of the peptide are of particular interest because these bulky side chains must interact with the membranes strongly and participate in the channel formation and cation transport. The importance of the trypotphan side chains has been demonstrated by the observations that the cation conductivity decreases upon substitution of one or all of the tryptophan residues by phenylalanine or tyrosine (Bamberg et al., 1976; Prasad et al., 1983; Heitz et al., 1982; Trudelle & Heitz, 1987) and also upon photolysis of the tryptophan rings (Busath & Waldbillig, 1983; Jones et al., 1986).

Raman spectroscopy is useful in studying the structures of peptides incorporated into lipid membranes. The information obtainable by this spectroscopic method includes the conformation of the peptide main chain, structures and environments of side chains, and conformational changes of lipid molecules induced by peptide incorporation. Several Raman spectroscopic studies have been carried out on gramicidin A–lipid systems to elucidate the backbone structure of gramicidin A (Rothschild & Stanley, 1975; Faiman & Long, 1976; Iqbal & Weidekamm, 1980; Naik & Krimm, 1984, 1986; Aslanian et al., 1986; Short et al., 1987) or the effects of gramicidin A on the gel to liquid-crystalline phase transitions of the lipids (Weidekamm et al., 1977; Susi et al., 1979). However, there is no systematic study on the tryptophan side chains, whose Raman bands predominate the spectrum of gramicidin A.

In this work, we have made Raman spectroscopic studies on the structure of gramicidin A incorporated into phospholipid liposomes, paying special attention to the environments and the conformations of the tryptophan side chains. The hydrophobic interaction of the indole ring with surrounding lipid molecules is monitored by using a Fermi doublet at 1360 and 1340 cm^{-1}, whose intensity ratio is known to be sensitive to such interactions (Harada et al., 1986; Miura et al., 1988). Water accessibility to the N_1H sites of the indole rings is studied by suspending the gramicidin A incorporated liposomes in D_2O and then recording the intensity of the 1385-cm^{-1} band characteristic of N_1-deuteriated tryptophan (Takesada et al., 1976; Miura et al., 1988) as a function of time. From the curve of intensity growth, it is possible to determine the number of tryptophan side chains accessible to water. Another Raman band used here is a strong band around 1550 cm^{-1}, whose frequency has recently been found to reflect the torsional angle $\chi^{2,1}$ of the $C_\alpha C_\beta$–C_3C_2 linkage (Miura et al., 1989). The frequency of this band provides the average torsional angle for the four tryptophans, and the band width reflects the distribution in the torsional angles. Effects of membrane thickness and cation binding on the hydrophobic interaction, water accessibility, and conformation are also examined by changing the length of hydrocarbon chains of the lipid or by preparing the liposomes in the presence of Na^+ ions.

Materials and Methods

Materials. Gramicidin isolated from *Bacillus brevis*, dilauroyl-L-α-phosphatidylcholine (DLPC,[1] 99%), dimyristoyl-L-α-phosphatidylcholine (DMPC, 99+%), and dipalmitoyl-L-α-phosphatidylcholine (DPPC, 99+%) were purchased from Sigma Chemical Co. The phospholipids were used without further purification. The natural gramicidin, a mixture of gramicidins A (80%), B (5%), and C (15%) (Killian et al., 1987), was recrystallized from methanol twice to remove fluorescent impurities, followed by vacuum evaporation of the solvent contained in the crystals. The less abundant gramicidin species, in which Trp-11 is replaced by a phenylalanine (gramicidin B) or a tyrosine residue (gramicidin C), was not detected in the Raman spectra, and we regarded the natural mixture as gramicidin A. A 500-MHz NMR analysis gave a tryptophan:phenylalanine:tyrosine ratio of 96:1:3 for the recrystallized gramicidin. N-Deuteriated gramicidin A was obtained by three-times recrystallization from CH_3OD, and the Raman spectrum of the crystal showed complete H–D exchange.

Sample Preparation. Gramicidin-containing liposomes were prepared as follows. Typically, 2.5 mg of gramicidin A and 8 mg of phosphatidylcholine (molar ratio ~1:9) were dissolved in 5 mL of chloroform (99%). The solutes were spread as a thin layer onto the wall of a 100-mL round-bottom flask by drying under vacuum. Excess drying time (>10 h) was taken to ensure complete removal of the solvent. Deionized water (3 mL) was then added to the flask and the lipid was hydrated under vortexing. The opaque suspension was sonicated for 10–20 min by using an ultrasonic generator with a tip probe (Nihonseiki Co., US-50). The hydration and sonication were performed at 60 °C, which is above the gel to liquid-crystalline phase transition temperatures of the lipids (DLPC, 3.3 °C; DMPC, 23.8 °C; DPPC, 41.3 °C; Huang et al., 1982). After sonication, the suspension was centrifuged to sediment traces of light-scattering multilamellar aggregate and titanium particles from the tip probe. Aliquots of the clear supernatant were used for circular dichroism (CD) measurement after 50-fold dilution in deionized water. The concentration of liposome in the supernatant was not high enough to serve as a sample of Raman spectral measurement, and therefore the supernatant was concentrated to a volume of ~0.1 mL by centrifugal filtration (700*g*) with a membrane filter (Amicon, Centriflo, CF25, molecular weight cutoff 25 000) under the phase transition temperature of the lipid. This ultrafiltration could filter out gramicidin molecules uncoated with the lipid or trapped in small micelles, if any. The lipid content in the liposomes was determined by phosphate analysis (Rouser et al., 1966), and the gramicidin content was evaluated by measuring the absorbance at 281 nm and using a molar extinction coefficient of 22 500 M^{-1} cm^{-1} determined for methanol solution. The gramicidin:lipid ratio thus determined was practically equal to that of the initial mixture.

Liposomes without gramicidin were prepared in a way similar to that described above. For the preparation of liposomes in the presence of Na^+, 3 mL of 50 mM NaCl solution was used for hydration instead of deionized water. Since significant aggregation of liposomes occurred under ultrafiltration for DPPC, the cation-bound gramicidin channel was examined only in DLPC and DMPC liposomes.

For H–D exchange experiments, gramicidin-incorporated liposomes were first prepared in H_2O and concentrated to a small volume, and then a large excess of D_2O (more than 50 times in volume) was added to the suspension, which was

[1] Abbreviations: DLPC, dilauroyl-L-α-phosphatidylcholine; DMPC, dimyristoyl-L-α-phosphatidylcholine; DPPC, dipalmitoyl-L-α-phosphatidylcholine; CD, circular dichroism; DMSO, dimethyl sulfoxide; NMR, nuclear magnetic resonance.

subsequently concentrated again to ~0.1 mL by ultrafiltration.

Raman Spectra. Raman spectra of liposomes were excited with 488-nm radiation of an Ar ion laser (CR Model 52) and recorded on a JASCO CT-80D monochromator equipped with a multichannel detection system (Princeton Instruments, SMA). The liposome suspension was sealed in a glass tube (2 mm i.d.) and mounted on a brass block thermostated with a constant temperature circulating bath (Neslab Instruments). The temperature of the block was kept at 1 (DLPC), 10 (DMPC), or 23 °C (DPPC). Increasing the temperature above the phase transition of the lipid caused changes in lipid Raman bands due to increase in gauche conformation in the acyl chains, but no significant changes were found for the gramicidin bands. Raman spectra of crystalline gramicidin were recorded on a scanning Raman spectrometer (JEOL, 400D) equipped with an Ar ion laser (NEC, GLG-3300, 514.5 nm). In all the Raman measurements, the spectral slit width was 3–5 cm^{-1}, and wavenumber calibration was made with the spectrum of indene. Peak wavenumbers of sharp bands were reproducible within ±1 cm^{-1}.

Characterization of Peptide Conformation by CD Spectroscopy. CD spectra in the 200–300-nm region were recorded on a JASCO J-400X spectropolarimeter using a 10-mm cell at room temperature. The spectra generally showed positive maxima at 218 ($\theta \sim 1.7 \times 10^4$ per residue) and 238 nm ($\theta \sim 0.4 \times 10^4$), negative ellipticity below 206 nm, and a shallow minimum at 229 nm, providing evidence that the gramicidin molecules were in the channel conformation (Urry et al., 1979; Wallace, 1986). The ellipticity of the 229-nm minimum varied from small negative to small positive with decreasing gramicidin:lipid ratio from 1:8 to 1:11, but no change was detected in the Raman spectra. Neither incubation of the liposomes at 65 °C for 24 h nor laser irradiation for Raman measurement changed the CD spectra significantly, indicating that the stable channel conformation was already formed in the liposomes and remained during the Raman measurement. Liposomes prepared by cosolubilizing the peptide and lipid in trifluoroethanol, which has recently been reported to be a good solvent to obtain the channel conformation (LoGrasso et al., 1988), gave the CD spectra similar to those of the liposomes prepared with chloroform. Raman spectra were also identical for the two preparation methods.

Results

Raman Spectroscopic Characterization of the Channel Structure. The Raman spectrum of gramicidin incorporated into DMPC liposomes is compared with that of crystalline gramicidin in Figure 1. In the solid state (Figure 1a), gramicidin takes double-stranded β-helical dimer conformation (Langs, 1988), and the amide I and III vibrations (Naik & Krimm, 1986) are observed at 1682 (I, shoulder), 1666 (I), 1283 (III), and 1232 cm^{-1} (III, broad). Similar spectral features in the amide I and III regions were observed for 10 mM dioxane (or dioxane-d_8) solution (spectrum not shown), in which gramicidin is known to form double-stranded β helices (Arseniev et al., 1984). In the Raman spectrum of the gramicidin–DMPC system (Figure 1b), the amide I bands are obscured by overlap of a strong H_2O band at 1639 cm^{-1}, and only a weak shoulder is seen at 1666 cm^{-1}. In the amide III region, on the other hand, two bands that lose intensity on N-deuteriation are observed at 1258 and 1233 cm^{-1} with comparable intensity. The frequencies of the two amide III bands are close to those found for a dilute dimethyl sulfoxide (DMSO) solution (1259 and 1237 cm^{-1}; Iqbal & Weidekamm, 1980), although the higher frequency band is stronger than the lower frequency one in DMSO solution. This intensity

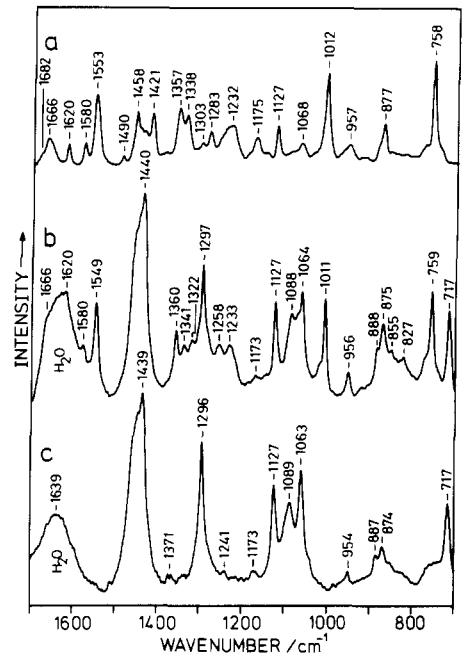

FIGURE 1: Raman spectra of crystalline gramicidin A (a), gramicidin A incorporated DMPC liposomes (molar ratio ca. 1:9) (b), and DMPC liposomes (c).

difference may be ascribed to small structural differences between the membrane-bound state and the DMSO solution. Actually, it has been reported that the gramicidin backbone in DMSO solution is also a single-stranded β helix but with conformational fluctuations involving local breaking of intramolecular hydrogen bonds (Hawkes et al., 1987). The 1283-cm^{-1} amide III band observed for crystalline gramicidin is absent in the spectrum of DMSO solution, whereas, in the gramicidin–DMPC spectrum, a shoulder at 1285 cm^{-1} is seen on the tail of a strong band at 1297 cm^{-1} due to the CH_2 twisting mode of the lipid (Gaber et al., 1978). Most of the intensity of this shoulder is certainly ascribed to the lipid vibration as seen in Figure 1c. However, a small contribution from the amide III vibration cannot be neglected because N-deuteriation reduced the intensity of the shoulder to some extent. The amide III contribution to this shoulder suggests that the conformation of the single-stranded helix is tighter in the membrane channel state than in the DMSO solution, and some amide groups are strongly hydrogen bonded, resulting in high-frequency amide III modes.

Besides the amide bands, many Raman bands assignable to tryptophan side chain vibrations (Iqbal & Weidekamm, 1980; Naik & Krimm, 1986; Takeuchi & Harada, 1986) are seen in the spectrum of crystalline gramicidin. The tryptophan Raman bands are also seen in the spectrum of the gramicidin–DMPC system. Among them, the bands at 1549, 1360, 1341, 1011, and 759 cm^{-1} are clearly observed without interference from the lipid bands. On going from the solid to the membrane-bound state, significant spectral change occurs in two frequency regions. The 1553-cm^{-1} band of the solid shifts to 1549 cm^{-1} in the membrane-bound state and the band width (full width at half-maximum) decreases from 17 to 12 cm^{-1}. The frequency of this tryptophan vibration has recently been found to vary from 1542 to 1557 cm^{-1} as a function of the absolute value of the $C_\alpha C_\beta$–C_3C_2 torsional angle ($\chi^{2,1}$) in the 60–120° range (Miura et al., 1989). According to the relationship, the average $|\chi^{2,1}|$ angle over the four tryptophan side chains of gramicidin is 99° in the solid state and 90° in the membrane-bound state. To deduce the distribution of the torsional angles from the bandwidth, we have measured the

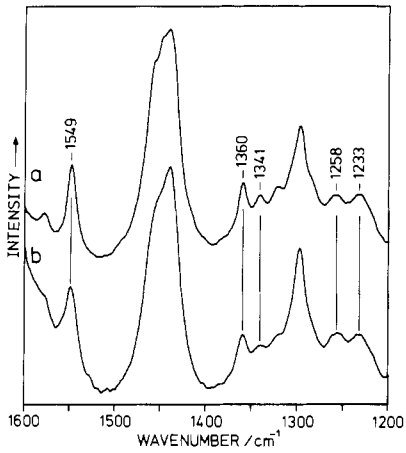

FIGURE 2: Raman spectra of gramicidin A incorporated into DLPC liposomes (a) and DPPC liposomes (b) in the 1600–1200-cm^{-1} region. The spectra below 1200 cm^{-1} are practically the same as the spectrum for DMPC liposomes (Figure 1b).

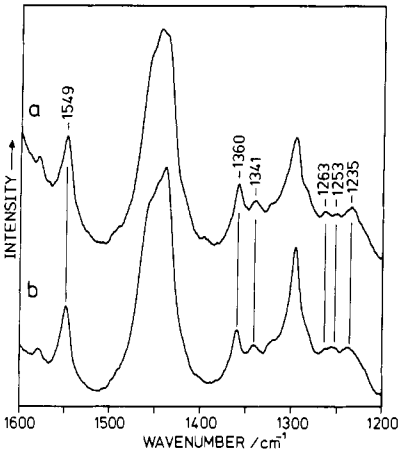

FIGURE 3: Raman spectra of gramicidin A incorporated into DLPC liposomes (a) and DMPC liposomes (b) in the presence of 50 mM Na^+.

bandwidth for compounds containing only one tryptophan ring such as L-tryptophan and found that the intrinsic bandwidth of a single tryptophan ring is 12 ± 1 cm^{-1}, which is comparable with that of gramicidin in the liposomes. Thus, it is concluded that all the four tryptophan side chains of gramicidin have $|\chi^{2,1}|$ angles very close to 90° in the membrane channel state. This contrasts with a significant distribution of the torsional angles in the solid state as judged from the broad feature of the 1553-cm^{-1} band.

Another spectral change is noticed in the intensity ratio of a doublet in the 1360–1335-cm^{-1} region. This doublet arises from Fermi resonance, and the intensity ratio I(high-frequency band)/I(low-frequency band) is known to reflect the strength of hydrophobic interaction of the indole ring with surrounding molecules, the ratio being greater for stronger hydrophobic interactions (Harada et al., 1986; Miura et al., 1988). In the solid-state spectrum, the 1357-cm^{-1} band is a little stronger than the 1338-cm^{-1} band, indicating that the tryptophan side chains are located in hydrophobic environments but the interactions are not so strong. This may be related to the crystal structure that the indole ring planes of neighboring helices are mostly orthogonal to one another (Langs, 1988). In the gramicidin–DMPC spectrum, on the other hand, the 1360-cm^{-1} band is much stronger than the 1341-cm^{-1} band, and it is concluded that most of the four tryptophan side chains are located in hydrophobic environments and strongly interacting with the acyl chains of the lipid.

Incorporation of gramicidin seems to affect the lipid structure. The 1296-cm^{-1} CH_2 twisting band becomes a little weaker in the presence of gramicidin as compared with the C–N symmetric stretching band of the choline group at 717 cm^{-1} (Akutsu et al., 1981). Likewise, in the C–C stretching region, the intensities at 1127 and 1063 cm^{-1} decrease even though they are overlapped by gramicidin bands. The 1127- and 1063-cm^{-1} bands of the lipid arise from all-trans hydrocarbon chains, and their intensity decreases together with that of the 1296-cm^{-1} band indicate localized conformational changes from trans to gauche about C–C bonds (Gaber et al., 1978). This observation is consistent with that of Susi et al. (1979) and indicates that gramicidin weakly perturbs the lipid bilayer structure by increasing the gauche content in the hydrocarbon chain region.

Effects of Membrane Thickness. Figure 2 shows the Raman spectra of gramicidin channel incorporated into DLPC and DPPC liposomes in the 1600–1200-cm^{-1} region for comparison with that of DMPC liposomes (Figure 1b). The acyl chains in these lipids contain 12 (DLPC), 14 (DMPC), and 16 (DPPC) carbon atoms, respectively, and the thickness of the nonpolar region of the lipid bilayer increases in this order. The tryptophan conformation marker band, which was observed at 1549 cm^{-1} in DMPC liposomes, is seen at the same frequency irrespective of the bilayer thickness. Its bandwidth shows no significant change on going from DMPC to DLPC (12 cm^{-1}) or DPPC (13 cm^{-1}). Thus, the $|\chi^{2,1}|$ angles of the four tryptophan side chains must be independent of the membrane thickness and remain close to 90°. On the other hand, the hydrophobic interactions of the tryptophan side chains with the lipid molecules appear to increase with the membrane thickness. The intensity ratio $I(1360)/I(1341)$ is smaller in DLPC and a little larger in DPPC than in DMPC. This result can be explained by assuming that one of the four tryptophans is located near the interface of nonpolar and polar regions of the bilayer and the hydrophobic interaction of that tryptophan is strong in DMPC and DPPC and weak in DLPC. The spectral features in the amide III region are very similar to one another for the three lipid systems, indicating that the backbone conformation of the channel does not depend on the membrane thickness.

Cation Binding Effect. To find the effects of cation on the structure of the gramicidin channel, we have incorporated gramicidin into liposomes in the presence of 50 mM Na^+. The Raman spectra of Na^+-bound gramicidin in DLPC and DMPC liposomes are shown in Figure 3. The tryptophan band at 1549 cm^{-1} changes neither in frequency nor in bandwidth upon cation binding. The $I(1360)/I(1341)$ ratio does not show any significant change either. Thus, the $|\chi^{2,1}|$ angles and the hydrophobic interactions remain unchanged in the cation-bound state. On the other hand, an effect of cation binding is seen clearly in the amide III region. Although the low-frequency component at 1233 cm^{-1} does not show a significant frequency shift, the high-frequency component at 1258 cm^{-1} splits into two bands peaking at 1263 and 1253 cm^{-1}. This splitting suggests that the backbone structure of the gramicidin channel in the cation-bound state differs partly from that in the cation-free state. Possibly some amide NH···O hydrogen bonds become stronger and others weaker.

Water Accessibility to the Indole N_1H Sites. If a tryptophan side chain is buried deep in the phospholipid bilayer, water molecules hardly approach the side chain. On the other hand, if the side chain is located near the surface of the bilayer, water molecules can reach the N_1H site of the indole ring and the N_1H proton exchanges with the water proton. This exchange rate can be monitored by using D_2O instead of H_2O

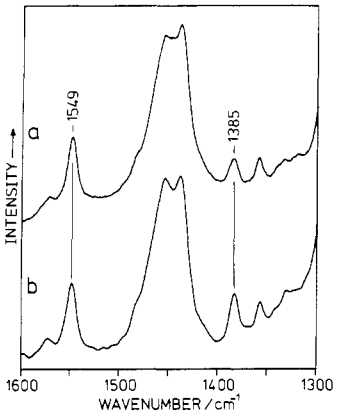

FIGURE 4: Raman spectra of gramicidin A incorporated into DMPC liposomes and then suspended in D_2O (3 h after suspension) (a) and predeuteriated gramicidin A incorporated into DMPC liposomes by using D_2O as the dispersion medium (b).

Table I: Deuterium Exchange Kinetics of the Tryptophan N_1 Protons of Gramicidin A Incorporated into Phospholipid Liposomes

lipid	half-time for exchange[a] (h)		
	Trp(1)	Trp(2)	Trp(3)
cation-free state			
DLPC	1.1 ± 0.5	1.1 ± 0.5	3.2 ± 0.4
DMPC	0.8 ± 0.3	0.8 ± 0.3	6.5 ± 0.5
DPPC	0.7 ± 0.3	2.5 ± 0.3	9.7 ± 0.7
Na^+-bound state			
DLPC	0.8 ± 0.3	2.0 ± 0.3	
DMPC	0.6 ± 0.2	2.8 ± 0.2	

[a] Obtained by least-squares analysis using a sum of three or two exponential functions of the $1 - \exp(-t/\tau)$ form, where t is the time (h) and $\tau \ln 2$ is the half-time for exchange.

as the dispersion medium. Here, we have examined the water (D_2O) accessibility to the four tryptophan side chains of gramicidin channels in phospholipid bilayers by the following method. First, we prepared gramicidin-incorporated liposomes in H_2O and then suspended the liposomes in D_2O as described under Materials and Methods. The Raman spectra of such liposomes were recorded at time intervals. A typical Raman spectrum in the course of H–D exchange is shown in Figure 4a, which was recorded for a DMPC dispersion 3 h after suspension in D_2O. Figure 4b shows the spectrum of a D_2O suspension of DMPC liposomes containing predeuteriated gramicidin, in which all four tryptophans are already N-deuteriated. In both of the spectra, the 1385-cm^{-1} band is characteristic of the N-deuteriated indole ring (Takesada et al., 1976) and the 1549-cm^{-1} band serves as an intensity standard because this tryptophan band is not affected by any of the membrane thickness, cation binding, and deuteriation. The integrated intensity ratio $I(1385)/I(1549)$ in Figure 4a is 55% of that in Figure 4b, indicating that 2.2 tryptophan side chains per molecule are H–D exchanged at a time of 3 h. The number of N-deuteriated tryptophan side chains thus obtained is plotted in Figure 5 as a function of time after suspension in D_2O for DLPC, DMPC, and DPPC liposomes in the absence of cation and for DLPC and DMPC liposomes in the presence of 50 mM Na^+. The curves in this figure show the least-squares fits with multiple-exponential functions. The half-time for H–D exchange obtained by the least-squares analysis is given in Table I for three exchangeable tryptophans [Trp(1), Trp(2), and Trp(3) in order of decreasing water accessibility] in the cation-free state and two tryptophans [Trp(1) and Trp(2)] in the cation-bound state.

The membrane thickness affects the water accessibility significantly as shown in Figure 5 and Table I. In DLPC and

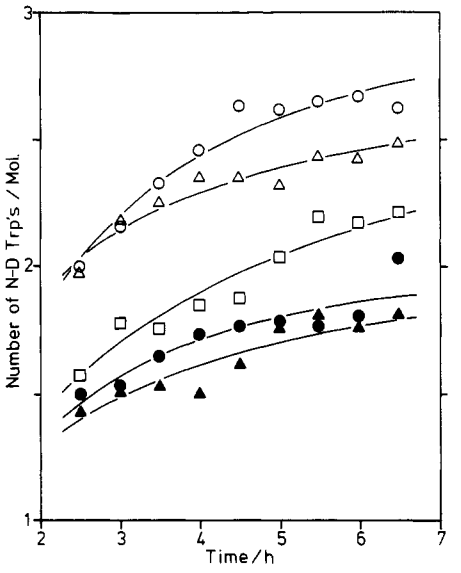

FIGURE 5: Number of N_1-deuteriated tryptophan side chains per molecule as a function of time after the dispersion medium was changed from H_2O to D_2O. Gramicidin A is incorporated into DLPC (circle), DMPC (triangle), or DPPC (square) liposomes. Open and solid symbols represent the results in the absence and presence of 50 mM Na^+, respectively.

DMPC, two of four tryptophans, Trp(1) and Trp(2), are deuteriated within 2.5 h (a dead time for sample preparation), and the deuteriation of the third tryptophan, Trp(3), proceeds more slowly. The increase in membrane thickness from DLPC to DMPC lowers the exchange rate of Trp(3), but the effects on the rates of Trp(1) and Trp(2) are insignificant. In DPPC, on the other hand, the H–D exchange of both Trp(2) and Trp(3) becomes much slower than in DLPC and DMPC. In all these lipid bilayers, the fourth tryptophan, Trp(4), is hardly reached by D_2O molecules, indicating that this side chain is deeply buried in the bilayer interior. It is interesting to note that the four tryptophans have water accessibilities significantly different from one another in the DPPC bilayers.

In the presence of Na^+, Trp(1) is readily N-deuteriated, whereas the water accessibility to Trp(2) is reduced greatly in both cases of DLPC and DMPC liposomes. Trp(3) becomes inaccessible on the time scale of hours, and Trp(4) remains inaccessible. These experimental results indicate that the cation binding induces the movements of the N_1H sites of Trp(2) and Trp(3) toward the bilayer center.

Discussion

Raman spectroscopy has provided information on the hydrophobic interactions, water accessibilities, and $|\chi^{2,1}|$ angles of the tryptophan side chains of gramicidin A incorporated into phospholipid bilayers. The strength of hydrophobic interaction depends on the degree of contact between the indole ring and the hydrocarbon chains of the lipid. The water accessibility of a tryptophan side chain indicates how deeply the N_1H site is buried in the bilayer. The orientation of an indole ring relative to the amide backbone is determined by two torsional angles, χ^1 about C_α–C_β and $\chi^{2,1}$ about C_β–C_3. The $|\chi^{2,1}|$ angle obtained by Raman spectroscopy produces limitations on the possible ring orientations. Here we will discuss the structure of gramicidin channel on the basis of the experimental results described above.

According to the head-to-head dimerized model of gramicidin channel, four tryptophan side chains (Trp-9, -11, -13, and -15) in the C-terminal half of each monomer are located near the entrance of the transmembrane channel, and their hydrophobic interactions with the lipid hydrocarbon chains

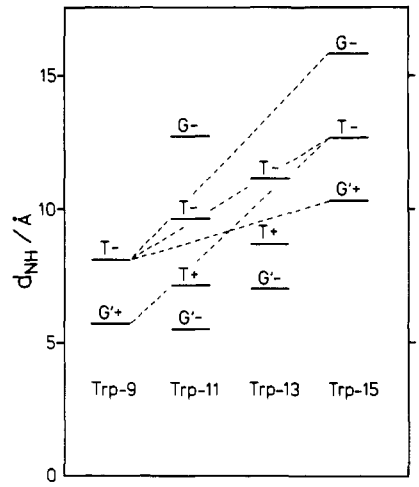

FIGURE 6: Distance of the N_1H proton (d_{NH}) along the channel axis measured from the channel center for Trp-9, -11, -13, and -15 in the possible conformations. The conformational pairs possible for Trp-9 and Trp-15 are connected by broken lines.

are expected to change with the thickness of the lipid bilayer. On the other hand, if the channel is formed by the tail-to-tail (carboxyl-to-carboxyl) dimerization, all the tryptophans would be buried near the bilayer center and the hydrophobic interactions would not be affected by the membrane thickness. The strength of hydrophobic interaction monitored by the Raman intensity ratio $I(1360)/I(1341)$ increased with increase of the thickness. This observation is consistent with the currently accepted head-to-head dimerization model but not with the tail-to-tail model.

Venkatachalam and Urry (1983) made conformational energy calculations on the head-to-head dimer and presented the lowest energy structure for the peptide backbone and side chains. The peptide backbone consists of two left-handed β helices with 6.2 residues per turn, and the side chains are oriented to minimize the steric conflict with the backbone and with the other side chains, particularly at positions one or six residues apart. Besides the lowest energy structure, many other side-chain conformations are energetically possible, as pointed out in their paper and by Roux and Karplus (1988). Such metastable conformational states may be important in considering the structure of a peptide embedded in membranes because peptide–membrane interactions can alter the order of stability for conformations of comparable energies. Here we focus on the conformations of tryptophan side chains. The χ^1 angle of a tryptophan side chain usually takes 180° (T), 60° (G), or −60° (G′), and this may also be the case of gramicidin. The $\chi^{2,1}$ angle has been determined by the present study to be 90° (+) or −90° (−). With these notations for the torsional angles, the possible tryptophan conformations proposed by Venkatachalam and Urry (1983) are represented by T+, G′−, T−, and G− for Trp-11, T+, G′−, and T− for Trp-13, and T–T−, T–G−, G′+T−, and T–G′+ for the pair of Trp-9 and Trp-15. The pairwise restriction on the Trp-9 and Trp-15 conformations arises from the balance of steric repulsion and attractive force between the two rings separated by one helix pitch. Thus, there are 48 conformational combinations to be examined for consistency with the water accessibility data.

The positions of the N_1H proton in the possible conformations were calculated for each tryptophan by using the structural parameters of Venkatachlam and Urry (1983) except the $\chi^{2,1}$ values, which were fixed to ±90° instead of the original values of ±60° or −120°. Figure 6 shows the distances, d_{NH}, of the N_1H protons measured along the helix axis from the center of head-to-head dimer junction. When the gramicidin channel is incorporated into a phospholipid bilayer, N_1H protons with large d_{NH} values are likely to be highly accessible to water, since they may be exposed to the hydrophilic region or located near the interface of the hydrophilic and hydrophobic regions, which contains transient structural defects capable of accommodating water molecules (Deamer & Bramhall, 1986). On the other hand, protons with small d_{NH} values are expected to be buried in the hydrophobic region. For such an N_1H site, the accessibility to water molecules penetrating from the outer aqueous phase may be distinctively low and decrease with decrease of d_{NH}. In this way, the water accessibility can be correlated with d_{NH}. As shown in Figure 5 and Table I, the four tryptophans of gramicidin have water accessibilities clearly different from one another when the channel is incorporated into DPPC bilayers. This fact indicates that any two tryptophans do not have close d_{NH} values. As seen in Figure 6, the difference in d_{NH} would be very small (0.2 Å) between Trp-9 and Trp-11 if they take the G′+G′− combination. Another example of improbable combinations is T+G′− for Trp-11 and Trp-13. Examination of all 48 conformational combinations shows that the minimum difference in d_{NH} is less than 1 Å for 32 combinations. The T–T+T+T− combination for Trp-9–Trp-15, which corresponds to the lowest energy structure of Venkatachalam and Urry (1983), also belongs to this category, and the N_1H sites of Trp-9 and Trp-13 are separated only by 0.6 Å. Such a small difference in d_{NH} does not seem to account for the significant differences in water accessibility characteristics among the tryptophan side chains. Accordingly, 16 combinations remain as the possible tryptophan conformations of the gramicidin channel.

Further limitations on the possible conformations are provided by the dependence of water accessibility on the membrane thickness. The thickness of the hydrophobic region of the bilayer decreases with decrease of the hydrocarbon chain length of the lipid, which results in a movement of the boundary of hydrophobic region toward the bilayer center. Trp(2) has a low accessibility (half-time for H–D exchange, 2.5 h) in DPPC, whereas it becomes highly accessible (half-time, ca. 1 h) in DMPC. This change in water accessibility is understood if the boundary shifts from outside to inside the N_1H site of Trp(2) on going from DPPC to DMPC. The DMPC bilayer is thinner than the DPPC bilayer by 4.1–4.3 Å (Janiak et al., 1976), suggesting an inward shift of ca. 2 Å for the boundary in each layer. Analogously, on going from DMPC to DLPC, the boundary is expected to further shift by ca. 2 Å toward the bilayer center. If the separation between Trp(2) and Trp(3) is less than this shift, Trp(3) would be outside the boundary in DLPC and become highly accessible to water. Actually, however, Trp(3) remains hardly accessible (half-time, 3.2 h) in DLPC. The separation in d_{NH} between Trp(2) and Trp(3) is thus required to be more than 2 Å. Of the 16 possible combinations, only the following 6 conformations satisfy the requirement: T–G–G′–G−, T–G–G′–G′+, T–G′–T–T−, T–G′–G–G−, G′+T+T–T−, and G′+T–G′–T−. The values of d_{NH} for these conformations are plotted in Figure 7.

Upon Na^+ binding, the H–D exchange rates of Trp(2) and Trp(3) decreases significantly and one of the amide III bands splits into two bands. Since the other amide III band does not show any significant change and CD spectroscopy has evidenced that the helical structure of the channel undergoes no major change upon cation binding (Wallace et al., 1981), the effects of Na^+ binding observed in the Raman spectra are associated with local change in the channel structure. A ^{13}C

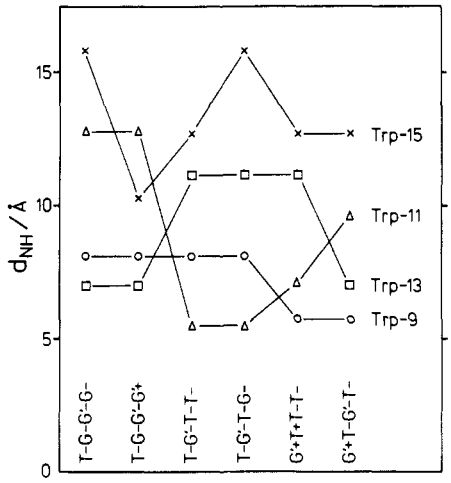

FIGURE 7: Plot of the d_{NH} values for Trp-9, -11, -13, and -15 in six possible conformational combinations.

NMR study on the ion-induced chemical shifts for the carbonyl carbons has shown that the cation-binding site is located near the Trp-11 and Trp-13 carbonyls (Urry et al., 1982a). Molecular dynamics calculations on the cation binding (Mackay et al., 1984) have demonstrated that the carbonyl bonds near the binding site deflect toward the cation in the channel pore, which results in movements of side chains in the distorted portion. Therefore, it is reasonable to correlate the Raman spectral changes with changes in the backbone and side-chain structure localized around Trp-11 and Trp-13. The splitting of the amide III band is thus ascribed to distortion of the helical structure around Trp-11 and Trp-13 and the decreases in water accessibility of Trp(2) and Trp(3) to the movements of Trp-11 and Trp-13 toward the bilayer center. Of the six conformations given in Figure 7, only the G'+T+T-T- and G'+T-G'-T- conformations shown in Figure 8 have Trp-11 and Trp-13 at the positions of Trp(2) and Trp(3). In the G'+T+T-T- conformation, Trp(2) and Trp(3) are assigned to Trp-13 and Trp-11, respectively, and in the G'+T-G'-T- conformation the assignment is reversed. Trp(1) and Trp(4) are assigned to Trp-15 and Trp-9, respectively, in both conformations. It is most likely that one of the two conformations represents the dominant orientation of the tryptophan side chains in the gramicidin A channel. Further discrimination of the two conformers is, however, impossible at present, and this problem is left for future studies employing new techniques such as selective isotopic labeling of individual tryptophans, in particular Trp-11 and Trp-13.

Single-channel conductance studies have revealed that there are various low-conductance channel states in addition to the major high-conductance states (Busath & Szabo, 1981). Such low-conductance channels convert reversibly to the major channels and are suggested to differ from the major channels in side-chain conformations (Urry et al., 1981; Busath & Szabo, 1988). The present models for the tryptophan conformations do not exclude the possibility that other tryptophan conformations are taken in some low-conductance states. Conformational conversion of tryptophan side chains, however, would encounter higher energy barriers than do the other smaller side chains such as valine and leucine. This may be particularly serious in the membrane environments, because the tryptophan side chains are strongly interacting with the hydrocarbon chains of the lipid as shown by Raman spectroscopy. The observation that the H–D exchange kinetics of tryptophan side chains can be expressed by simple exponential decay functions does not favor the coexistence of diverse tryptophan conformations, either. It is rather likely that the

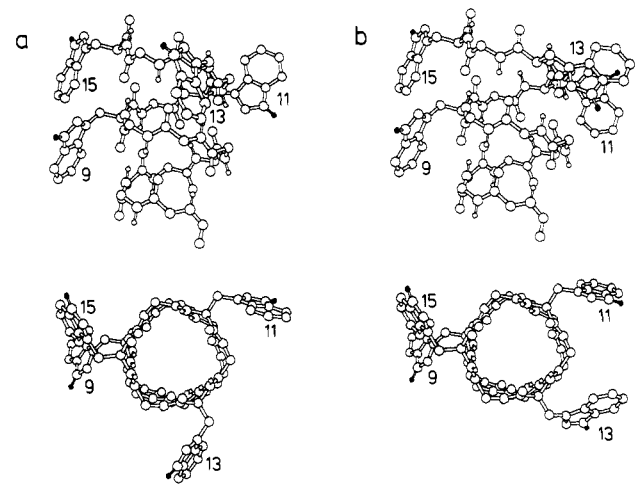

FIGURE 8: Two models for the tryptophans orientation in the gramicidin A channel. Tryptophan conformations are G'+T+T-T- (a) and G'+T-G'-T- (b). Views normal to the helix axis (upper) and from the channel entrance (lower) are shown for half of the channel (monomer). The N_1H protons of tryptophan side chains are filled in. The ethanolamide group at the channel entrance and the side chains other than tryptophans are omitted.

low-conductance states differ from the major channel states in conformations of valine and leucine side chains and/or of the ethanolamide group at the entrance of the channel. Selective isotopic labeling of individual tryptophan side chains will be useful in determining whether the conductance heterogeneity arises from conformational heterogeneity of the tryptophan side chains or of the other parts of gramicidin.

In summary, Raman spectroscopy has provided unique information on the environments and conformations of the tryptophan side chains of gramicidin A incorporated into phospholipid bilayers. Most of the four tryptophan side chains are strongly interacting with the lipid hydrocarbon chains, and the interaction strength for the rest depends on the bilayer thickness. The N_1H site of one tryptophan is easily accessible to water molecules, and that of another is inaccessible. The accessibilities for the remaining two depend on the bilayer thickness and whether the cation is bound or not. The $\chi^{2,1}$ angles of all four tryptophans are fixed to ±90° in both the cation-free and cation-bound states. Two models, which are consistent with the Raman data, are proposed for the dominant tryptophan conformation. The models may be useful in studying the mechanism of cation transport by the gramicidin channel.

Registry No. L-Trp, 73-22-3; DLPC, 18194-25-7; DMPC, 18194-24-6; DPPC, 63-89-8; Na, 7440-23-5; gramicidin A, 11029-61-1.

References

Akutsu, H. (1981) *Biochemistry 20*, 7359–7366.

Arseniev, A. S., Bystrov, V. F., Ivanov, V. T., & Ovchinnikov, Y. A. (1984) *FEBS Lett. 165*, 51–56.

Aslanian, D., Nègrerie, M., & Chambert, R. (1986) *Eur. J. Biochem. 160*, 395–400.

Bamberg, E., Noda, K., Gross, E., & Läuger, P. (1976) *Biochim. Biophys. Acta 419*, 223–228.

Busath, D., & Szabo, G. (1981) *Nature 294*, 371–373.

Busath, D. D., & Waldbillig, R. C. (1983) *Biochim. Biophys. Acta 736*, 28–38.

Busath, D., & Szabo, G. (1988) *Biophys. J. 53*, 689–695.

Deamer, D. W., & Bramhall, J. (1986) *Chem. Phys. Lipids 40*, 167–188.

Faiman, R., & Long, D. A. (1976) *J. Raman Spectrosc. 5*, 87–92.

Finkelstein, A., & Andersen, O. S. (1981) *J. Membr. Biol. 59*, 155–171.
Gaber, B. P., Yager, P., & Peticolas, W. L. (1978) *Biophys. J. 21*, 161–176.
Harada, I., Miura, T., & Takeuchi, H. (1986) *Spectrochim. Acta 42A*, 307–312.
Hawkes, G. E., Lian, L. Y.; Randall, E. W., Sales, K. D., & Curzon, E. H. (1987) *Eur. J. Biochem. 166*, 437–445.
Heitz, F., Spach, G., & Trudelle, Y. (1982) *Biophys. J. 39*, 87–89.
Hladky, S. B., & Haydon, D. A. (1972) *Biochim. Biophys. Acta 274*, 294–312.
Huang, C., Lapides, J. R., & Levin, I. W. (1982) *J. Am. Chem. Soc. 104*, 5926–5930.
Iqbal, Z., & Weidekamm, E. (1980) *Arch. Biochem. Biophys. 202*, 639–649.
Janiak, M. J., Small, D. M., & Shipley, G. G. (1976) *Biochemistry 15*, 4575–4580.
Jones, D., Hayon, E., & Busath, D. (1986) *Biochim. Biophys. Acta 861*, 62–66.
Killian, J. A., Burger, K. N. J., & De Kruijff, B. (1987) *Biochim. Biophys. Acta 897*, 269–284.
Langs, D. A. (1988) *Science 241*, 188–191.
LoGrasso, P. V., Moll III, F., & Gross, T. A. (1988) *Biophys. J. 54*, 259–267.
Mackay, D. H. J., Berens, P. H., Wilson, K. R., & Hagler, A. T. (1984) *Biophys. J. 46*, 229–248.
Miura, T., Takeuchi, H., & Harada, I. (1988) *Biochemistry 27*, 88–94.
Miura, T., Takeuchi, H., & Harada, I. (1989) *J. Raman Spectrosc. 20*, 667–671.
Myers, V. B., & Haydon, D. A. (1972) *Biochim. Biophys. Acta 274*, 313–322.
Naik, V. M., & Krimm, S. (1984) *Biochem. Biophys. Res. Commun. 125*, 919–925.
Naik, V. M., & Krimm, S. (1986) *Biophys. J. 49*, 1147–1154.
Prasad, K. U., Trapane, T. L., Busath, D., Szabo, G., & Uryy, D. W. (1983) *Int. J. Pept. Protein Res. 22*, 341–347.
Rosenberg, P. A., & Finkelstein, A. (1978) *J. Gen. Physiol. 72*, 341–350.
Rothschild, K. R., & Stanley, H. E. (1975) *Am. J. Clin. Pathol. 63*, 695–649.
Rouser, G., Siakotos, A. N., & Fleischer, S. (1966) *Lipids 1*, 85–86.
Roux, B., & Karplus, M. (1988) *Biophys. J. 53*, 297–309.
Sarges, R., & Witkop, B. (1964) *J. Am. Chem. Soc. 86*, 1862–1863.
Short, K. W., Wallace, B. A., Myers, R. A., Fodor, S. P. A., & Dunker, A. K. (1987) *Biochemistry 26*, 557–562.
Susi, H., Sampugna, J., Hampson, J. W., & Ard, J. S. (1979) *Biochemistry 18*, 297–301.
Takesada, H., Nakanishi, M., Hirakawa, A. Y., & Tsuboi, M. (1976) *Biopolymers 15*, 1929–1938.
Takeuchi, H., & Harada, I. (1986) *Spectrochim. Acta 42A*, 1069–1078.
Trudelle, Y., & Heitz, F. (1987) *Int. J. Pept. Protein Res. 30*, 163–169.
Urry, D. W. (1971) *Proc. Natl. Acad. Sci. U.S.A. 68*, 672–676.
Urry, D. W., Spisni, A., & Khaled, M. A. (1979) *Biochim. Biophys. Acta 88*, 940–949.
Urry, D. W., Venkatachalam, C. M., Prasad, K. U., Bradley, R. J., Parenti-Castelli, G., & Lenz, G. (1981) *Int. J. Quantum Chem. Quantum Biol. Symp. 8*, 385–399.
Urry, D. W., Prasad, K. U., & Trapane, T. L. (1982a) *Proc. Natl. Acad. Sci. U.S.A. 79*, 390–394.
Urry, D. W., Walker, J. T., & Trapane, T. L. (1982b) *J. Membr. Biol. 69*, 225–231.
Urry, D. W., Trapane, T. L., & Prasad, K. U. (1983) *Science 221*, 1064–1067.
Venkatachalam, C. M., & Urry, D. W. (1983) *J. Comput. Chem. 4*, 461–469.
Wallace, B. A. (1986) *Biophys. J. 49*, 295–306.
Wallace, B. A., Veatch, W. R., & Blout, E. R. (1981) *Biochemistry 20*, 5754–5760.
Weidekamm, E., Bamberg, E., Brdiczka, D., Wildermuth, G., Macco, F., Lehmann, W., & Weber, R. (1977) *Biochim. Biophys. Acta 464*, 442–447.
Weinstein, S., Wallace, B. A., Morrow, J. S., & Veatch, W. R. (1980) *J. Mol. Biol. 143*, 1–19.